SLEEP, 2023, 1–11
https://doi.org/10.1093/sleep/zsac286
Advance access publication 30 November 2022
Original Article

Original Article

Dementia detection from brain activity during sleep

Elissa M. Ye[1,2], Haoqi Sun[1,2], Parimala V. Krishnamurthy[1,2], Noor Adra[1,2], Wolfgang Ganglberger[1,2], Robert J. Thomas[3], Alice D. Lam[1,†] and M. Brandon Westover[1,2,†,*]

[1]Department of Neurology, Massachusetts General Hospital, Boston, MA, USA,
[2]Clinical Data Animation Center (CDAC), Boston, MA, USA and
[3]Division of Pulmonary, Critical Care and Sleep, Department of Medicine, Beth Israel Deaconess Medical Center, Boston, MA, USA

†Co-senior authors.
*Corresponding author. M. Brandon Westover, Department of Neurology, Massachusetts General Hospital, Boston, MA, USA. Email: mwestover@mgh.harvard.edu.

Abstract

Study Objectives: Dementia is a growing cause of disability and loss of independence in the elderly, yet remains largely underdiagnosed. Early detection and classification of dementia can help close this diagnostic gap and improve management of disease progression. Altered oscillations in brain activity during sleep are an early feature of neurodegenerative diseases and be used to identify those on the verge of cognitive decline.

Methods: Our observational cross-sectional study used a clinical dataset of 10 784 polysomnography from 8044 participants. Sleep macro- and micro-structural features were extracted from the electroencephalogram (EEG). Microstructural features were engineered from spectral band powers, EEG coherence, spindle, and slow oscillations. Participants were classified as dementia (DEM), mild cognitive impairment (MCI), or cognitively normal (CN) based on clinical diagnosis, Montreal Cognitive Assessment, Mini-Mental State Exam scores, clinical dementia rating, and prescribed medications. We trained logistic regression, support vector machine, and random forest models to classify patients into DEM, MCI, and CN groups.

Results: For discriminating DEM versus CN, the best model achieved an area under receiver operating characteristic curve (AUROC) of 0.78 and area under precision-recall curve (AUPRC) of 0.22. For discriminating MCI versus CN, the best model achieved an AUROC of 0.73 and AUPRC of 0.18. For discriminating DEM or MCI versus CN, the best model achieved an AUROC of 0.76 and AUPRC of 0.32.

Conclusions: Our dementia classification algorithms show promise for incorporating dementia screening techniques using routine sleep EEG. The findings strengthen the concept of sleep as a window into neurodegenerative diseases.

Key words: dementia; EEG; sleep; machine learning; biomarker

Graphical Abstract

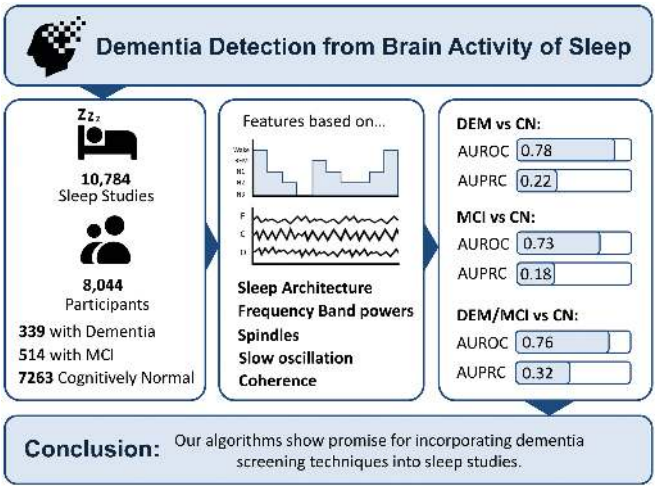

Submitted for publication: September 21, 2022; **Revised:** November 10, 2022

Statement of Significance

Using sleep EEG data from more than 8,000 sleep clinic patients, we extracted various macro- and micro-structural features and trained machine learning models to identify patients with mild cognitive impairment and dementia. With a significantly large dataset and comprehensive set of features, our study has demonstrated the discriminative power of brain activity during sleep for detecting dementia. There is promise for using home-based wearable EEG to routinely screen individuals for dementia, which can help close the diagnostic gap.

Introduction

Among people aged 65 years and older in the United States, 11% have dementia of various etiologies [1] and 16% have mild cognitive impairment [2] (MCI). Despite its prevalence, dementia remains largely undiagnosed [3, 4], with its symptoms being difficult to differentiate from normal consequences of aging. Early diagnosis can identify people at risk for complications [5] and improve prognosis [6] with early intervention.

Currently, clinical diagnosis of dementia relies on the clinical history, cognitive screening tests (e.g. Montreal Cognitive Assessment [MoCA], Mini-Mental State Examination [MMSE]), laboratory tests, and neuroimaging studies such as brain magnetic resonance imaging and positron emission tomography. However, these tests are typically performed when an underlying neurodegenerative disease has already manifested long enough to cause noticeable cognitive decline. A method to detect deteriorating brain health with high sensitivity before significant progression of cognitive decline is thus highly desirable.

Electroencephalography (EEG) is a low-cost, noninvasive technology that measures brain electrical activity. Quantitative EEG metrics have been identified as a potential biomarker in early detection of dementia [7–10]. Several studies have used spectral and/or nonlinear features of the awake EEG to detect signs of dementia [11–15]. However, few studies have evaluated the discriminative power of sleep EEG features, although sleep disturbances are recognized as risk factors and early clinical symptoms of neurodegenerative disorders. Sleep architecture (macro-structure) changes, including increases in sleep fragmentation, number of awakenings (NA), rapid eye movement (REM) latency, and reductions in slow-wave and REM sleep, are often reported in dementia [16–18]. Micro-structural changes, including EEG slowing [19], decreased θ and δ band power during slow-wave sleep [20], and decreased EEG coherence [21, 22], and deterioration of sleep spindles during non-REM (NREM) sleep [16, 23], have been observed in demented patients as well. The power ratio of α sub-bands $\alpha 3/\alpha 2$ is also indicative of MCI to dementia conversion [24, 25]. Given the vast amount of literature supporting the relationship between, sleep EEG patterns and dementia, we believe that sleep EEG is a promising non-invasive measure source for potential indicators of underlying neurodegenerative pathology.

In prior work, we reported that a sleep EEG-based brain age index increased monotonically from nondementia to dementia subpopulations [26]. Here, we investigated the discriminative power of macro- and micro-structural changes in brain activity during sleep for detection of dementia and MCI. To explore the relationship between sleep and early neurodegeneration and dementia, we identified top sleep EEG features that differentiated those with diagnosed dementia of different etiologies (DEM) and MCI patients from cognitively normal (CN) patients. We examined the spectral profiles and age-dependency of sleep features across diagnostic groups. To measure the utility of sleep EEG features in discriminating between DEM, MCI, and CN individuals, we developed algorithms to perform binary classification (DEM vs CN; MCI vs CN; DEM/MCI vs CN) and evaluated their performance. We hypothesized that features extracted from sleep EEG and machine learning models based on them could significantly discriminate DEM and MCI participants from CN participants.

Methods

Dataset

This is an observational cross-sectional study. The Massachusetts General Brigham Institutional Review Board approved all study procedures and waived the requirement for informed consent for this retrospective study. We included participants who underwent polysomnogram(s) (PSG) for clinical purposes in the Sleep Laboratory at Massachusetts General Hospital from 2009 to 2019. PSGs were recorded and scored adhering to American Academy of Sleep Medicine guidelines. The dataset included 22 991 PSGs from 17 279 participants and contained three major types of sleep tests: diagnostic, full-night titration, and split-night titration. For split-night titration studies, only the PSG from the diagnostic segment was included. Each PSG was annotated by an experienced sleep technician. Every 30-second nonoverlapping epoch was classified as one of five stages: Wake (W), NREM stage 1 (N1), NREM stage 2 (N2), NREM stage 3 (N3), and REM.

Clinical data extraction

Clinical data, including participant demographics, encounter diagnoses, medications, and clinical notes, were extracted for all participants from questionnaires completed before the sleep study and from electronic medical records. Scores for the clinical dementia rating (CDR) global scale, MMSE [27], and MoCA [28], when available, were extracted from clinical notes using in-house software. Obstructive sleep apnea was defined as apnea-hypopnea index ≥5 and based on the PSG report. Medical diagnoses were extracted from documentation in the electronic health record.

Dementia staging

Table 1 shows the inclusion and exclusion criteria for Dementia (DEM), MCI, and CN groups. Inclusion criteria were based on data entered in the medical record before the sleep study or at most one year after the sleep study unless otherwise stated. Keywords are listed in Supplementary Table S1. We excluded any encounter diagnosis containing the keyword "family history." Participants were assigned to a group using the criteria met closest to the date of sleep study. If a participant satisfied criteria for dementia but later received a CDR ≤ 0.5, MMSE > 25, or MoCA score > 20, we classified them as MCI. If a participant had multiple sleep studies, we analyzed each one independently, and assigned the dementia stage with respect to date of each sleep study.

To develop the criteria, we labeled 123 cases into DEM, MCI, and CN groups based on expert chart review and iteratively improved our criteria using a series of error analyses and rule refinement. We settled on our criteria that predicted DEM and

MCI with a false positive rate of 0% and discriminated between them with accuracy >80%.

EEG preprocessing

For each PSG recording, six EEG channels (F3-M2, F4-M1, C3-M2, C4-M1, O1-M2, and O2-M1) were resampled to 200 Hz, notch-filtered at 60 Hz, and bandpass filtered at 0.5 to 20 Hz. To minimize nonphysiological artifacts, all 30-second epochs with maximum absolute amplitude greater than 500 uV, and epochs containing more than 2 s of flat signal (standard deviation less than 0.2 uV), were excluded. We excluded epochs with strong narrow-band spectral artifacts (such as electrocardiogram noise) by checking if the second-order difference of spectrum between 4 and 20 Hz exceeded an empirically determined threshold.

Macro-structure sleep features

Sleep architecture features were obtained from hypnograms, including total resting time (TRT), total sleep time (TST), duration of sleep stages, percent of time spent in sleep stages, sleep efficiency index (SEI, or TST/TRT), sleep onset latency (time to first sleep stage), wake after sleep onset, REM latency, NA, number of stage shifts to N1 from NREM/REM sleep (NSS), and sleep fragmentation index (SFI, or [NA + NSS]/TST).

Micro-structural sleep features

We extracted EEG microstructure data from each 30-second epoch for each EEG channel, using the same features from Sun *et al.* [29]. In the time domain, we calculated the line length, kurtosis, and sample entropy to quantify signal complexity. In the frequency domain, we calculated the minimum, maximum, mean, and standard deviation across 2-second sub-epochs within each 30-second epoch, for relative δ, θ, and α band powers, δ/θ, δ/α, and θ/α power ratios, and kurtosis of δ, θ, α, and σ bands. All features were calculated as averages across left and corresponding right channels, separately for frontal, central, and occipital channels. Features were averaged across all epochs falling into the same sleep stage. For participants with missing sleep stages, features for the missing sleep stages were imputed with the average of the 10 closest participants based on Euclidean distance of features from other sleep stages. This resulted in 510 features.

Individual EEG frequencies and alpha sub-band powers

Individual EEG frequencies and α sub-band powers were extracted from epochs in the Wake and N1 stages. We calculated the θ/α transition frequency (TF) as the minimum power in the θ frequency range and the individual alpha frequency (IAF) as the maximum power following TF in the extended α range (5–14 Hz) [25]. Using these individual EEG frequencies as anchors, we defined the α sub-band ranges: α1 (TF to TF-IAF midpoint), α2 (TF-IAF midpoint to IAF), and α3 (IAF to IAF + 2 Hz) [25]. We computed the power spectral density of α1, α2, and α3 sub-bands and the α3/α2 power ratio for each stage and region (frontal, central, and occipital, each averaged across left and right sides). This resulted in 36 features.

Spindle and slow-wave oscillation features

Spindle and slow oscillation (SO) patterns during N2 sleep were detected using Luna software [30] using the following parameters: central frequency for spindle = 13.5 Hz (to nonspecifically capture both slow and fast spindles); wavelet cycle number = 12 (for better frequency resolution); and relative amplitude threshold for slow oscillation = 1.5 (empirically tuned to N2). This resulted in 228 features.

EEG coherence features

EEG coherence was defined as the magnitude squared coherence estimate of two discrete-time signals using Welch's method. EEG coherences were computed from each epoch across all channel pairs (15 combinations) and averaged for each frequency band (δ, θ, α, and σ). EEG coherences were then averaged across all epochs for each sleep stage. This resulted in 300 features.

Matching between groups

We matched participants in each group by sex and age using the DEM group as the reference for matching. For each DEM participant, we found matching individuals in each of the other groups, with the same sex and age within 5 years. The MCI group was oversampled with replacement due to its smaller size.

Comparison of EEG power spectra across groups

To compare spectra of DEM, MCI, and CN, we computed the spectrum for each 30-second epoch for all PSGs in the matched

Table 1. Inclusion and exclusion criteria for DEM, MCI, and CN groups

Group	Inclusion criteria
Dementia	• CDR global score ≥ 1 • MMSE score < 25 • MoCA score < 20 • ≥ 1 dementia medication with dementia diagnosis • ≥ 1 dementia diagnosis and ≥1 symptomatic diagnosis
MCI	• CDR global score = 0.5 • MMSE score between 25 and 27 • MoCA score between 20 and 26 • ≥1 dementia medication with MCI diagnosis • ≥1 MCI diagnosis and ≥1 symptomatic diagnosis
CN	• Does not belong to the dementia and MCI groups and has no dementia/MCI diagnosis
	Exclusion Criteria • Age < 50 years • Prior diagnosis of developmental delay, brain tumor, stroke, brain damage, and Down's syndrome

Participants were assigned to a group if they met at least one of the inclusion criteria and did not meet any of the exclusion criteria.

groups. For each participant, we averaged data from the frontal, central, and occipital channels respectively, and calculated the average spectra for each sleep stage. The participant-level spectra were then averaged across participants within each diagnostic group. For Wake, N1, and REM stages, we determined the IAF and TF for the average spectra for each group. For N2 and N3 stages, we determined the spindle peak frequency as the frequency at local maximum within the 10–15 Hz range. If no local maximum existed in that range, we defaulted to 13Hz. Significant differences in frequency and power were determined using one-way analysis of variance (ANOVA) and post hoc tests.

Statistical analysis

To evaluate differences in the proportion of medical diagnoses between DEM, MCI, and CN groups, we performed two-sample proportion z-tests comparing the prevalence of each medical diagnosis for DEM versus CN, and MCI versus CN.

To identify EEG features that discriminated DEM and MCI from CN, we standardized the features and analyzed the odds ratios (ORs) of logistic regression (LR) models on the matched groups. *p*-values were adjusted using the Benjamini-Hochberg procedure to correct for multiple comparisons.

To investigate how sleep features changed with age across groups, we used a linear model with interaction terms based on the following equation:

$$\begin{aligned}\text{Feature} = {} & \beta_0 + \beta_1 \cdot \text{Age} + \beta_2 \cdot \text{DEM} + \beta_3 \cdot \text{Age} \cdot \text{DEM} + \\ & \beta_4 \cdot \text{MCI} + \beta_5 \cdot \text{Age} \cdot \text{MCI}\end{aligned} \quad (1)$$

where DEM and MCI were coded as 1 if present and 0 otherwise. All sleep features were standardized, and missing values were imputed using *K*-nearest neighbors ($K = 10$). For each linear model term, we identified the top sleep features based on the significance and magnitude of their effect coefficients (β).

Machine learning classification

We created binary classification models to distinguish DEM, MCI, and CN groups based on sleep features (Figure 1). For binary classification, we created models to discriminate DEM versus CN, MCI versus CN, and DEM/MCI (combined) versus CN. We used three models: LR, support vector machine (SVM), and random forest (RF). For feature selection, we used ANOVA as a filter method to select features independently correlated with the dependent variable; and we used RF as a model-based feature selection method. To optimize and evaluate performance of the classifiers, we used nested fivefold cross-validation which incorporates hyperparameter tuning and out-of-sample performance estimation. Within each fold of the outer loops, we standardized the data and imputed missing values using k-nearest neighbor imputation with $K = 10$. Then, we applied the filter and wrapper methods for feature selection and tuned the classification model hyperparameters using grid search within the inner folds. The grid search used area under receiver operating characteristic (AUROC) as the metric to evaluate model performance and optimize hyperparameters. Performance of each optimized model was tested on the held-out data from the outer loop. We used area under precision-recall curve (AUPRC) as a complementary performance metric.

Due to the imbalanced nature of our dataset (DEM:MCI:CN = 1:1.5:22), we set a balanced class weight for all models, which adjusted weights to be inversely proportional to class frequencies. For LR models, we applied the elastic-net penalty and tuned hyperparameters C (inverse of regularization strength) and l1 ratio (elastic-net mixing parameter). To implement linear SVM, we used a stochastic gradient descent estimator with a hinge loss function and tuned the hyperparameter alpha (a constant that multiplies the regularization term). For RF models, we used the Gini impurity to measure the quality of splits and tuned hyperparameters for maximum tree depth, number of trees, and a complexity parameter used for minimal cost-complexity pruning.

Results

Baseline characteristics

After applying the exclusion criteria, our final dataset included 10 784 PSGs from 8044 participants. The median (interquartile range) age was 63 (56–70) years and 57% were male. By our criteria, 339 participants (449 PSGs) were categorized into the DEM group, 514 (672 PSGs) into the MCI group, and 7263 (9663 PSGs) into the CN group. When comparing DEM and MCI groups to the CN group, we found significant differences in proportion of participants with a history of mood disorders, anxiety disorders, diabetes, psychotic disorders, and alcoholism (**Table 2**). We found a significantly higher proportion of cardiovascular disease in DEM versus CN, but not MCI versus CN.

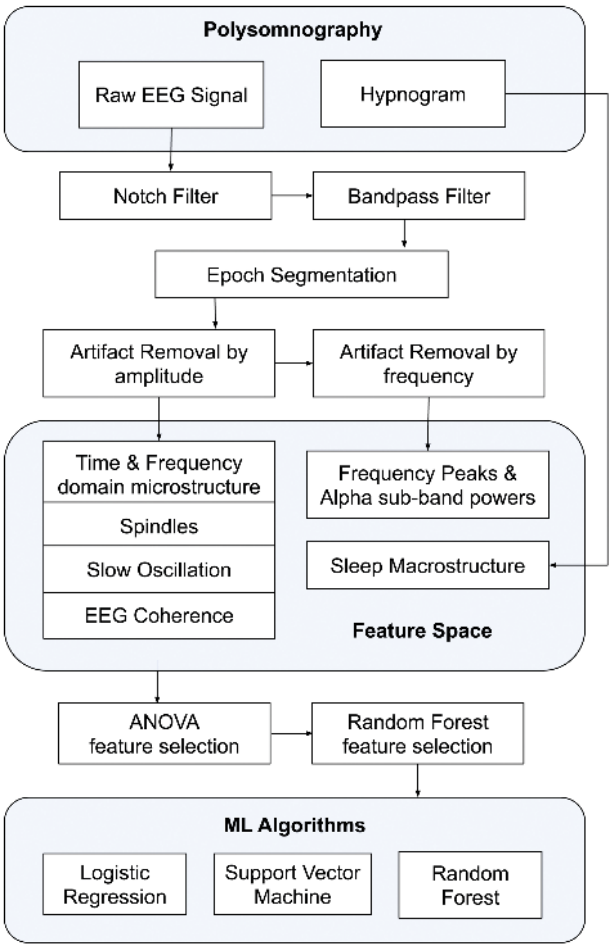

Figure 1. Flowchart of EEG preprocessing, feature engineering, feature selection, and model development pipeline.

Table 2. Summary of group characteristics

Characteristics	Total	CN	MCI	DEM
Number of PSGs	10 784	9663 (42%)	672 (2.92%)	449 (1.95%)
Number of participants	8116	7263	514	339
Age	63 (56–70)	62 (55–69)	69 (62–75)	72 (63–78)
Sex				
Female	4635 (43%)	4203 (43%)	249 (37%)	183 (41%)
Male	6137 (57%)	5449 (56%)	423 (63%)	265 (59%)
Ethnicity				
Asian	284 (3%)	252 (3%)	10 (1%)	22 (5%)
White	8643 (80%)	7718 (80%)	583 (87%)	342 (76%)
Black	547 (5%)	503 (5%)	27 (4%)	17 (4%)
Hispanic	297 (3%)	261 (3%)	18 (3%)	18 (4%)
Other/unknown	1013 (9%)	929 (10%)	34 (5%)	50 (11%)
Type of study				
Diagnostic	4610 (43%)	4147 (43%)	272 (40%)	191 (43%)
All night titration	3000 (28%)	2672 (28%)	200 (30%)	128 (29%)
Split night	3174 (30%)	2844 (30%)	200 (30%)	130 (29%)
Cardiovascular disease	8451 (78%)	7519 (78%)	539 (80%)	393 (88%)***
Obstructive sleep apnea	6401 (59%)	5700 (58%)	422 (63%)	279 (62%)
Mood disorder	5543 (51%)	4741 (49%)	485 (72%)***	317 (70%)***
Obesity	5393 (50%)	4855 (50%)	330 (49%)	208 (46%)
Insomnia	5175 (48%)	4611 (48%)	353 (53%)*	211 (47%)
Diabetes	4899 (45%)	4339 (45%)	335 (50%)*	225 (50%)*
Anxiety disorder	4602 (43%)	3913 (41%)	431 (64%)***	258 (57%)***
Psychotic disorder	1177 (11%)	823 (9%)	188 (28%)***	166 (37%)***
Alcoholism	1057 (9.8%)	880 (9%)	108 (16%)***	69 (15%)***

Percentage indicates proportion within each group or total. Interquartile range is indicated for age. For comorbid diseases, asterisks indicate a significant difference in proportion compared to CN group.
*$p < .05$. ***$p < .001$.

Top discriminative features for DEM, MCI, and CN groups

To assess which sleep features (from a feature space of 1066 features) most consistently differed between diagnostic groups, we calculated ORs and p-values based on LR models, using DEM or MCI as the case group and CN as the control group (Figure 2). For DEM versus CN, 499 features had significant ORs (177 associated with DEM and 322 associated with CN). For MCI versus CN, 386 features had significant ORs (95 associated with MCI and 291 associated with CN). The top discriminative features associated with DEM and MCI were related to θ and δ activity in W and N1 sleep, and features related to spindles and slow oscillations. For MCI, the associations with features related to θ and δ activity in W and N1 sleep were slightly weaker, whereas the associations with features related to spindles and slow oscillations were stronger. For DEM, we found more associations with features related to θ and δ band powers in REM sleep. When compared with DEM and MCI as a group, the CN group showed consistent associations with α features in W and N1 sleep, spindle features in N2 sleep, δ, θ, and α features in N2 and N3 sleep, and most feature types in REM sleep (Supplementary Figure S1).

Spectral analysis

Differences in IAF, TF, and spindle peaks from different sleep stages are shown in Figure 3. For this analysis, we plotted the average spectra in the occipital region. The occipital channels showed the most prominent fast spindle peaks, which have known impacts on Alzheimer's disease (AD) [31], compared to frontal (Supplementary Figure S2) and central channels (Supplementary Figure S3). found that TF power was greater for DEM when compared with CN for Wake ($p < .001$), N1 ($p < .001$), and REM (all $p < 0.01$). TF power was similarly greater for MCI when compared with CN for Wake ($p < .001$), N1 ($p < .001$), and REM ($p < .05$). The frequency of TF was significantly higher in DEM ($p < .05$) and MCI ($p < .001$) for N1 sleep. IAF was lower in the Wake, N1, and REM when comparing both DEM and MCI with CN ($p < .001$ for all). For N2 sleep, power at the average spindle peak frequency was significantly lower for DEM ($p < .01$), but not for MCI, when compared with CN. For N3, no significant differences in power spectra were observed at any frequency.

Relationship between sleep features, age, and diagnostic group

To evaluate the relationships between sleep features, age, and diagnostic group, we used a linear model with interaction terms

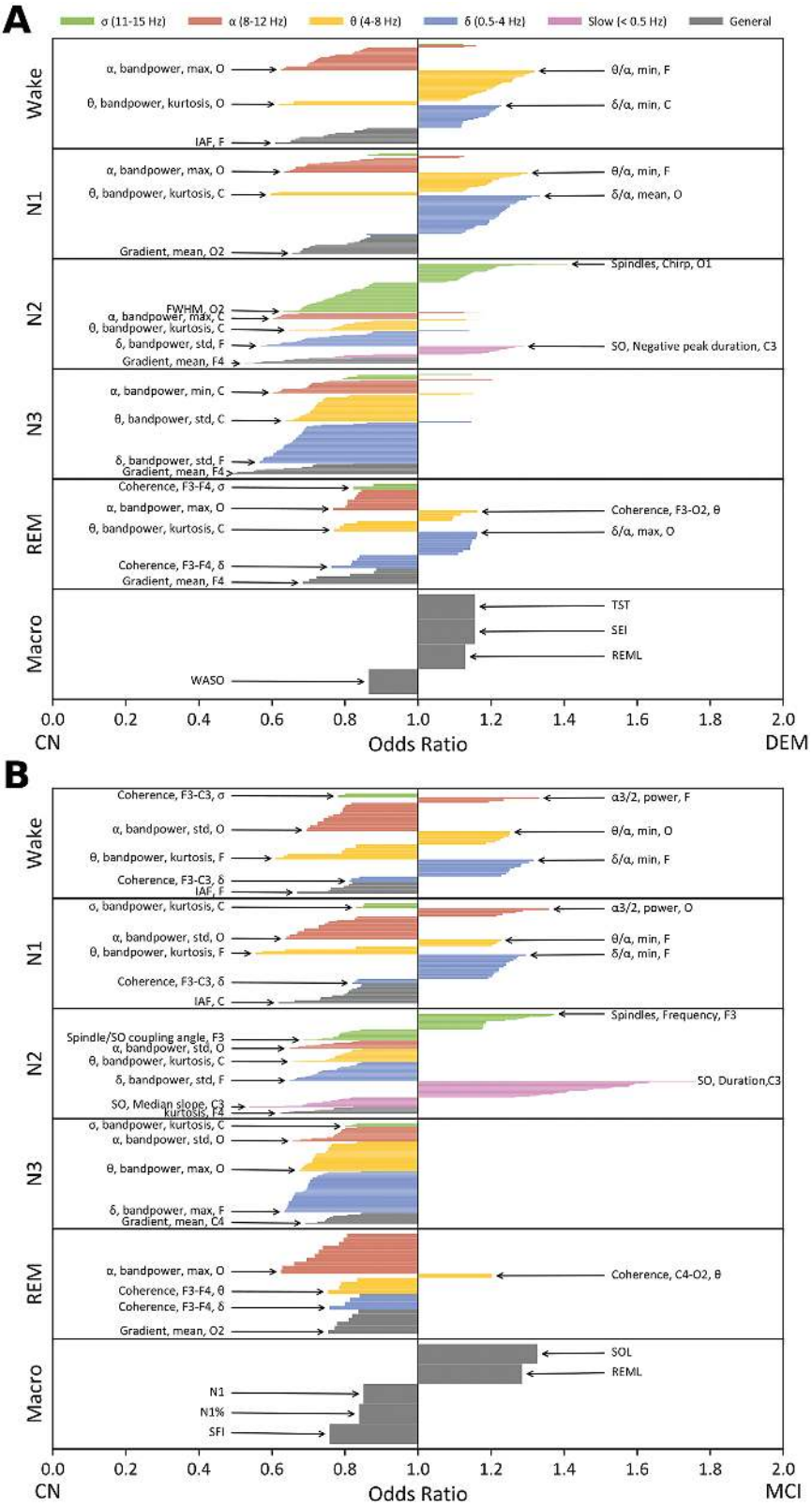

Figure 2. Top discriminative features for (A) DEM versus CN and (B) MCI versus CN based on OR. Only features with significant associations were included in the plot.

to model each sleep feature, based on participant age, diagnostic group (DEM and MCI), and interactions between age and diagnostic group (see Equation (1) in Methods section). Supplementary Table S2 lists features with the top 20 positive, significant coefficients for each term, and Supplementary Table S3 shows features with the top 20 negative, significant coefficients for each term.

The DEM term (β_2) had the largest positive effects on features related to θ band power in N1/Wake stages and the largest

negative effects on features related to δ band power in N2/N3 stages and kurtosis in N2. DEM × Age interaction term (β_3) had the largest positive effects on features related to spindles and the largest negative effects on features related to α band power and gradient mean in Wake/N1 stage. The MCI term (β_4) had the largest positive effects on features related to slow oscillations and the largest negative effects on features related to δ band power in N2/N3 stages. MCI × Age interaction (β_5) had the largest positive effects on features related to slow oscillation and negative effects on a heterogenous mix of other features, possibly due to having lower magnitude effects compared with other effect coefficients. Figure 4 illustrates the age-dependent effects across diagnostic groups for the top features associated with DEM, DEM × Age, MCI, and MCI × Age terms.

Dementia stage classification

We next evaluated the extent to which sleep features could be used to discriminate between DEM, MCI, and CN groups using machine learning models. On all tasks, performance of the three different machine learning methods (LR, SVM, and RF) were similar. Figure 5 shows the receiver operating characteristic (ROC) curves and precision-recall curves for binary classification tasks. For discriminating DEM versus CN, SVM had the best performance (by a small margin) with an AUROC of 0.78 and AUPRC of 0.22 (AUPRC for chance level performance = 0.04). For discriminating MCI versus CN, LR performed best with an AUROC of 0.73 and AUPRC of 0.18 (AUPRC for chance level performance = 0.06). For discriminating DEM/MCI versus CN, LR performed best with an AUROC of 0.76 and AUPRC of 0.32 (with chance level performance = 0.10). Supplementary Table S4 lists performance metrics for each classifier in detail.

Discussion

Our findings demonstrate that features derived from sleep EEG can be used to discriminate DEM, MCI, and CN groups. Out of 1066 sleep features, 177 features were positively and significantly associated with dementia, and 95 features were positively and significantly associated with MCI when compared with CN. Spectral analysis demonstrated observable differences in landmark frequencies across DEM, MCI, and CN groups. Some sleep features showed significant interaction effects between age and diagnostic group. Binary classifiers achieved decent AUROC and AUPRC scores for distinguishing DEM versus CN, MCI versus CN, and DEM/MCI versus CN.

The DEM, MCI, and CN groups have distinct associations with features in different sleep stages. DEM and MCI groups had discriminative features related to θ and δ activity in W and N1 sleep, compared with CN. Chiaramonti *et al.* [32] found that dementia was associated with high absolute power in θ and δ frequency bands. The θ/α ratio is also known to be higher in patients with dementia [33]. Features related to spindles and slow-wave oscillations were also important for distinguishing DEM/MCI and CN. Studies have shown that both AD and MCI have decreased spindle density in N2, likely related to memory consolidation facilitated by hippocampal-cortical interactions, compared to healthy controls [20, 23]. Moreover, reduced spindles may represent an early dysfunction related to tau, reflecting axonal damage or altered neuronal tau secretion, according

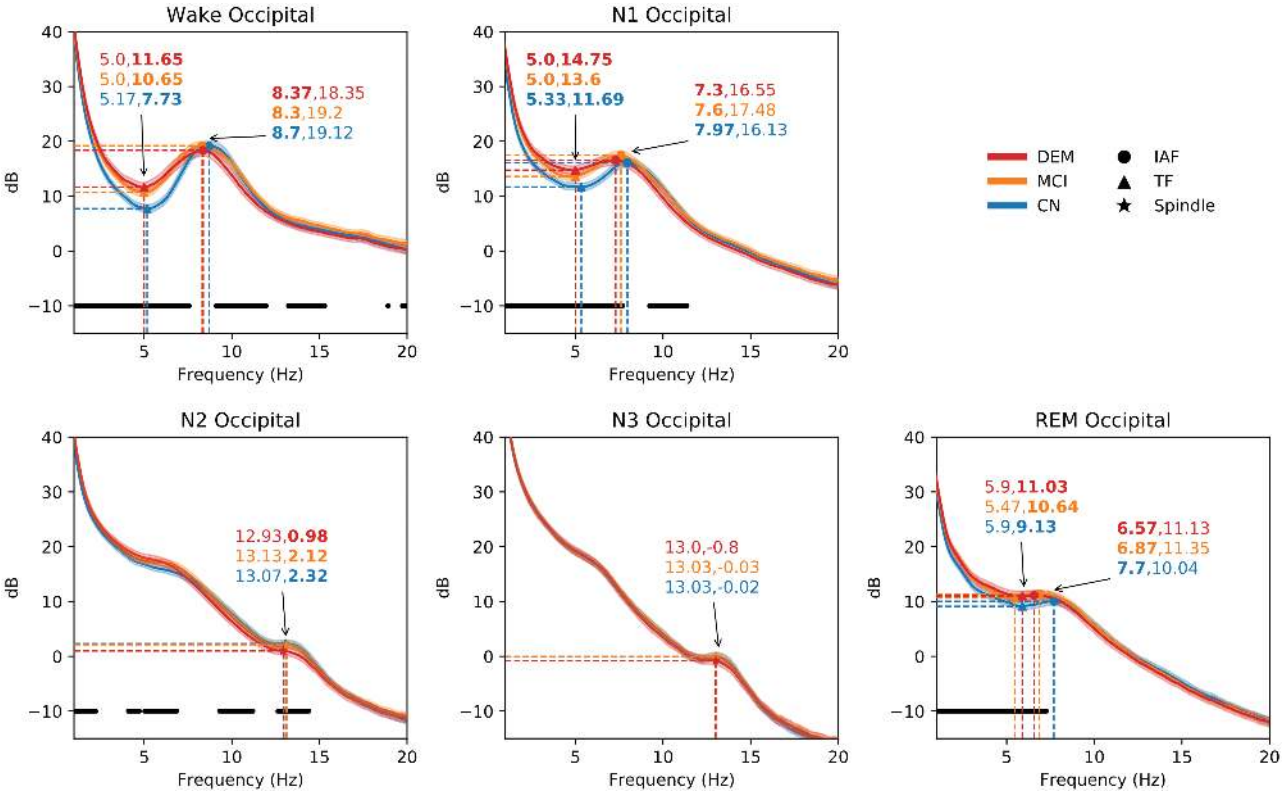

Figure 3. Comparison of occipital EEG power spectra between DEM, MCI, and CN groups, across different sleep stages. Data points representing the IAF, TF, and Spindle peaks are annotated as (frequency and power). Significance differences ($p < .05$ for ANOVA test) in frequency and power of landmarks are indicated in bold. Black line indicates significant differences in power spectra across groups at specific frequencies.

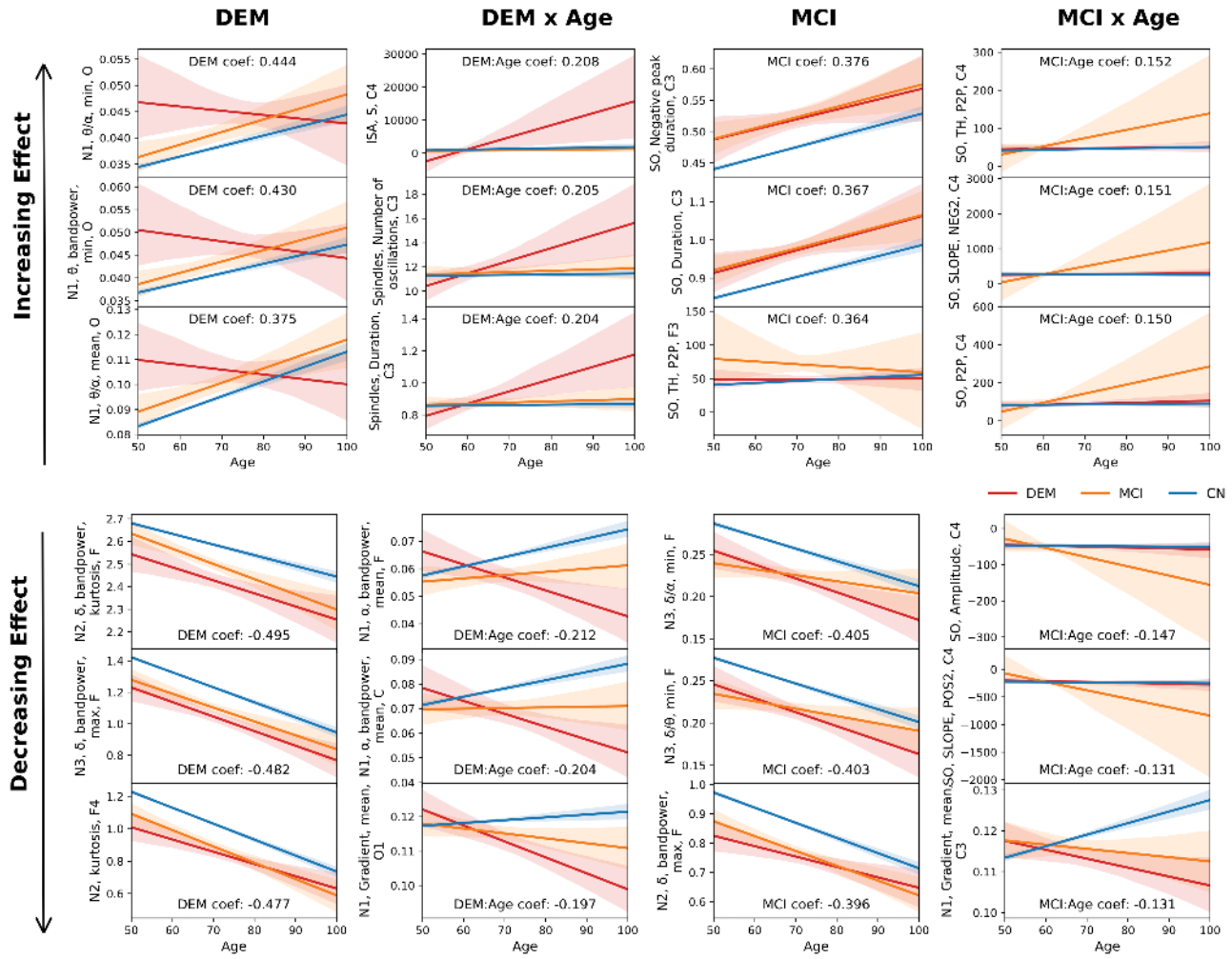

Figure 4. Regression plots of age versus features were selected using a linear model with interaction terms. The x-axis represents age and y-axis represents non-standardized feature values. Lines represent the best linear regression model fit and 95% confidence interval for DEM, MCI, and CN groups. Plots are arranged in columns by the effect coefficients used to choose the top features. Row of plots are sorted by increasing and decreasing effects. All features have $p < .001$ for each of their corresponding**β**. Integrated spindle activity (ISA) is based on the sum of normalized wavelet coefficients in the spindle interval.

to a study by Kam *et al.* [34]. Diminished Spindle-SO coupling and slow-wave amplitude are also known features of tau and β-amyloid plaques respectively [35]. DEM showed more associations with features related θ and δ in REM sleep, which may reflect REM sleep disturbances due to cholinergic dysfunction in dementia, consistent with prior studies in AD that evaluated slow frequency activity in REM [36, 37]. The MCI group had stronger associations with features related to slow oscillations when compared with the DEM group, which may suggest these features to be related to early stages of neurodegeneration. In W and N1 sleep, CN had prominent associations with most features related to α activity, which is correlated with hippocampal volume [38] and cognitive and memory performance [39]. In contrast, the power ratio of α3/α2, a known indicator of MCI to dementia conversion [24, 25] correlated with hippocampal atrophy [40], was found to be associated with MCI. The CN group's associations with δ, θ, and α features in N2/N3/REM sleep were expected as robust slow-wave and REM sleep features have known associations with preserved cognitive function [41].

Spectral analysis demonstrated significant differences in landmark spectral peak frequencies in all sleep stages when comparing DEM and MCI groups to age and sex-matched CN participants. The shifting of the IAF peaks to lower frequencies is typically a stable neurophysiological trait of aging and age-related neuroanatomical changes, such as degeneration of gray and white matter [42, 43]. Given that this shift was found in age-matched DEM and MCI groups, the observed α peak frequency slowing is likely due to progression of disease instead of normal aging. Consistent with our findings, Moretti *et al.* [25] observed slower IAF for Alzheimer's participants compared with normal. Tanabe *et al.* [44] also found that α peak frequency slowing was associated with amyloid and tau pathology impacts. The accentuated power at the θ and δ bands in W and N1 stages for both DEM and MCI groups has been observed previously [32]. Surprisingly, the difference in power was most pronounced at the TF. The accentuated power at TF is not often discussed as a characteristic of dementia, but our results show that this is an important predictor. Diminished spindle peaks in N2 for the DEM group are an indicator of decreased spindle power, which aligns with prior research that found reductions in spindle amplitude for AD participants [45, 46]. However, no differences in spindle peaks were observed for the MCI group, which may suggest that changes in spindles are more characteristic of later-stage dementia [47]. We found no significant differences in spectral analysis in N3, which suggests that spectral information in N3 is less informative as an indicator for dementia/MCI.

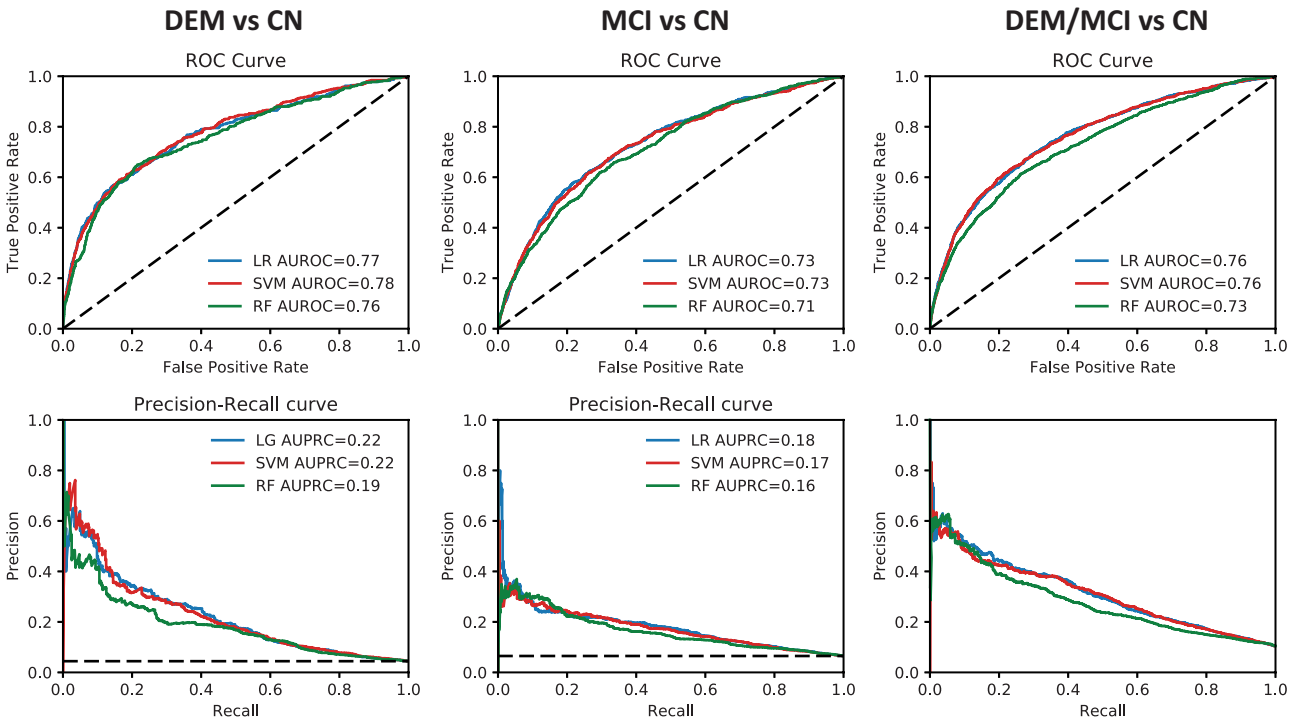

Figure 5. ROC curves and precision-recall curves of classifiers, DEM vs CN, MCI vs CN, and DEM/MCI vs CN, evaluated with nested cross-validation. Black dashed line represents chance level performance.

Results from our linear models revealed differences in feature change with age across DEM, MCI, and CN groups. The presence of dementia increased the features related to θ band power in N1/Wake stage, including θ/α band power ratio, a known marker of AD [33]. The increase in theta power in Wake/N1 stages is characteristic of elderly people with longitudinal cognitive decline and negatively correlated with hippocampal volume and perfusion level [48]. Dementia also decreased the features related to δ band power in N2/N3 stage, reflecting diminished slow-wave activity. Age-modulated effects of dementia increased features related to spindle activity, such as mean integrated spindle activity per spindle, number of oscillations per spindle, and spindle duration. These features captured specific morphological characteristics of the spindles, rather than the spindle density, which decreases with both normal aging and dementia [23]. Ktonas *et al.* [49] also found that spindles from dementia participants exhibit faster oscillations than controls, although we did not observe shorter spindle duration as they did. Features related to α band power in Wake/N1 stage decreased the most with age-modulated effects of dementia. This is expected as we know that α rhythms decrease as a function of age [50] and even more dramatically in dementia. The presence of MCI seems to increase features related to slow oscillations, including SO negative peak duration, duration, and peak-to-peak threshold. Increases in these SO features may reflect the age-related changes in morphology of slow-waves, namely longer duration depolarization and hyperpolarization processes [51], that may be accentuated by neurodegenerative diseases. Features that decreased the most with dementia were related to δ band power in N2/N3 stage, reflecting decreased slow-wave activity during slow-wave sleep. Similarly, features that decreased the most with MCI were related to δ band power in N2/N3 stage.

Our binary classification models achieved good performance overall on the DEM versus CN task. The MCI versus CN task performed comparatively worse, which was expected given that MCI is physiologically less distinctive than DEM. Some prior studies focusing on the same general problem using other datasets have reported higher discrimination [11–13, 52]. However, most of these have much smaller patient cohorts, thus it is unclear whether results generalize to larger and more diverse cohorts. Neto *et al.* [15] had a larger cohort size of 114 patients with AD and 114 with vascular dementia (VaD) patients and achieved performance similar to ours in discriminating dementia patients with AD (AUROC = 0.74) and VaD (AUROC = 0.77) from healthy controls. Prior studies have also used data from wake EEG recordings with dense EEG channels (about 20). Our study is unique in that we used sleep EEG, which better reflects autonomic physiology.

Limitations

There are several limitations to this study. First, our study was done using PSGs obtained from sleep clinics; the generalizability of our findings to populations warrants further study. Second, labeling of DEM and MCI groups relied on clinical diagnoses and cognitive screening tests, which were extracted from the electronic medical record, and did not include biomarker or neuropathologic confirmation. Third, our MCI and DEM groups likely included individuals with different underlying neurodegenerative diseases, such as Alzheimer's disease, VaD, frontotemporal dementia, and Lewy body dementia, that may each have distinct EEG signatures [53–56]. For our dataset, we were limited by the number of people with confirmed diagnoses of specific neurodegenerative diseases. Further study examining differences in EEG patterns across different neurodegenerative diseases may be informative to our research.

Conclusion

Our study shows that brain activity during sleep has the potential to detect features associated with dementia and contains

information that can help inform individual-level clinical decision-making. There is thus promise for clinical translation using home-based wearable EEG to routinely screen individuals for dementia and provide individual-level neuropathological estimates for diagnosis and monitoring of disease progression.

Supplementary Material

Supplementary material is available at *SLEEP* online.

Funding

MBW received grant support from the Glenn Foundation for Medical Research and American Federation for Aging Research through a Breakthroughs in Gerontology Grant, an American Academy of Sleep Medicine Foundation Strategic Research Award, National Institutes of Health (R01NS102190, R01NS102574, R01NS107291, RF1AG064312, RF1NS120947, R01AG073410, and R01HL161253), and National Science Foundation (2014431). RJT received grant support from an American Academy of Sleep Medicine Foundation Strategic Research Award, 1RF1AG064312. ADL received grants from National Institute of Neurological Disorders and Stroke K23 NS101037 and the American Academy of Neurology Institute.

Disclosure Statement

Financial Disclosure: MBW is a co-founder of Beacon Biosignals. RJT has (1) a licensed patent for ECG/PPG spectrogram, to MyCardio, LLC, for sleep quality and sleep apnea phenotyping, (2) unlicensed patent for CO_2 device for central sleep apnea; licensed patent for auto-CPAP algorithm (Devilbiss-Drive), (3) Consulting for Guidepoint Global, GLG Councils, and Jazz Pharmaceuticals, and (4) Medical Advisory Board for Beacon Biosignals. No other disclosures were reported.

Nonfinancial disclosure: No nonfinancial disclosure to report.

Conflict of Interest Statement: The authors have no conflict of interest.

References

1. Hudomiet P, *et al*. Dementia prevalence in the United States in 2000 and 2012: estimates based on a nationally representative study. *J Gerontol B Psychol Sci Soc Sci*. 2018;**73**:S10–S19. doi:10.1093/geronb/gbx169.
2. Petersen RC, *et al*. Practice guideline update summary: mild cognitive impairment report of the guideline development, dissemination, and implementation. *Neurology*. 2018;**90**(3):126–135. doi:10.1212/WNL.0000000000004826.
3. Amjad H, *et al*. Underdiagnosis of dementia: an observational study of patterns in diagnosis and awareness in US older adults. *J Gen Intern Med*. 2018;**33**(7):1131–1138. doi:10.1007/s11606-018-4377-y.
4. Lang L, *et al*. Prevalence and determinants of undetected dementia in the community: a systematic literature review and a meta-analysis. *BMJ Open*. 2017;**7**(2):e0111461–e0111468. doi:10.1136/bmjopen-2016-011146.
5. Ashford JW, *et al*. Should older adults be screened for dementia? It is important to screen for evidence of dementia!. *Alzheimers Dement*. 2007;**3**:75–80. doi:10.1016/j.jalz.2007.03.005.
6. Rasmussen J, *et al*. Alzheimer's disease – why we need early diagnosis. *Degener Neurol Neuromuscul Dis*. 2019;**9**:123–130. doi:10.2147/DNND.S228939.
7. Al-Qazzaz NK, *et al*. Role of EEG as biomarker in the early detection and classification of dementia. *ScientificWorldJournal*. 2014;**2014**:906038. doi:10.1155/2014/906038.
8. Babiloni C, *et al*. What electrophysiology tells us about Alzheimer's disease: a window into the synchronization and connectivity of brain neurons. *Neurobiol Aging*. 2020;**85**:58–73. doi:10.1016/j.neurobiolaging.2019.09.008.
9. Babiloni C, *et al*. Measures of resting state EEG rhythms for clinical trials in Alzheimer's disease: recommendations of an expert panel. *Alzheimers Dement*. 2021;**17**(9):1528–1553. doi:10.1002/alz.12311.
10. Snyder SM, *et al*. Addition of EEG improves accuracy of a logistic model that uses neuropsychological and cardiovascular factors to identify dementia and MCI. *Psychiatry Res*. 2011;**186**(1):97–102. doi:10.1016/j.psychres.2010.04.058.
11. Ruiz-Gómez SJ, *et al*. Automated multiclass classification of spontaneous EEG activity in Alzheimer's disease and mild cognitive impairment. *Entropy (Basel)*. 2018;**20**(1):351–315. doi:10.3390/e20010035.
12. Lehmann C, *et al*. Application and comparison of classification algorithms for recognition of Alzheimer's disease in electrical brain activity (EEG). *J Neurosci Methods*. 2007;**161**(2):342–350. doi:10.1016/j.jneumeth.2006.10.023.
13. Fiscon G, *et al*. Combining EEG signal processing with supervised methods for Alzheimer's patients classification. *BMC Med Inform Decis Mak*. 2018;**18**(1):1–10. doi:10.1186/s12911-018-0613-y.
14. Ieracitano C, *et al*. A Convolutional Neural Network approach for classification of dementia stages based on 2D-spectral representation of EEG recordings. *Neurocomputing*. 2019;**323**:96–107. doi:10.1016/j.neucom.2018.09.071.
15. Neto E, *et al*. Regularized linear discriminant analysis of EEG features in dementia patients. *Front Aging Neurosci*. 2016;**8**:1–10. doi:10.3389/fnagi.2016.00273.
16. Petit D, *et al*. Sleep and quantitative EEG in neurodegenerative disorders. *J Psychosom Res*. 2004;**56**(5):487–496. doi:10.1016/j.jpsychores.2004.02.001.
17. Sciences B, *et al*. Disturbances of sleep and cognitive functioning in patients with dementia. *Neurobiol Aging*. 1982;**3**:371–377.
18. Reynolds CFRI, *et al*. EEG sleep in elderly depressed, demented, and healthy subjects. *Biol Psychiatry*. 1985;**20**(1):431–442.
19. Montplaisir J, *et al*. Sleep disturbances and EEG slowing in Alzheimer's disease. *Sleep Res Online*. 1998;**1**(4):147–151.
20. Westerberg CE, *et al*. Concurrent impairments in sleep and memory in amnestic mild cognitive impairment. *J Int Neuropsychol Soc*. 2012;**18**(3):490–500. doi:10.1017/S135561771200001X.
21. Dunkin JJ, *et al*. Reduced EEG coherence in dementia: state or trait marker? *Biol Psychiatry*. 1994;**35**(11):870–879. doi:10.1016/0006-3223(94)90023-x.
22. Laptinskaya D, *et al*. Global EEG coherence as a marker for cognition in older adults at risk for dementia. *Psychophysiology*. 2020;**57**(4):1–13. doi:10.1111/psyp.13515.
23. Gorgoni M, *et al*. Parietal fast sleep spindle density decrease in alzheimer's disease and amnesic mild cognitive impairment. *Neural Plast*. 2016;**2016**:1–10. doi:10.1155/2016/8376108.
24. Moretti DV, *et al*. MCI patients' EEGs show group differences between those who progress and those who do not progress to AD. *Neurobiol Aging*. 2011;**32**(4):563–571. doi:10.1016/j.neurobiolaging.2009.04.003.
25. Moretti DV, *et al*. Individual analysis of EEG frequency and band power in mild Alzheimer's disease. *Clin Neurophysiol*. 2004;**115**(2):299–308. doi:10.1016/s1388-2457(03)00345-6.

26. Ye E, *et al.* Association of sleep electroencephalography-based brain age index with dementia. *JAMA Netw Open.* 2020;**3**(9):e2017357. doi:10.1001/jamanetworkopen.2020.17357.
27. Folstein MF, *et al.* "Mini-Mental State" a pratical method for grading the cognitive state of patients for the clinician. *Psychiatr Res.* 1975;**12**:189–198.
28. Nasreddine ZS, *et al.* The Montreal Cognitive Assessment, MoCA: a brief screening tool for mild cognitive impairment. *J Am Geriatr Soc.* 2005;**53**(4):695–699. doi:10.1111/j.1532-5415.2005.53221.x.
29. Sun H, *et al.* Brain age from the electroencephalogram of sleep. *Neurobiol Aging.* 2019;**74**:112–120. doi:10.1016/j.neurobiolaging.2018.10.016.
30. Purcell SM, *et al.* Characterizing sleep spindles in 11,630 individuals from the National Sleep Research Resource. *Nat Commun.* 2017;**8**(May):1–16. doi:10.1038/ncomms15930.
31. Rauchs G, *et al.* Is there a link between sleep changes and memory in Alzheimer's disease? *Neuroreport.* 2008;**19**(11):1159–1162. doi:10.1097/WNR.0b013e32830867c4.
32. Chiaramonti R, *et al.* Correlations of topographical EEG features with clinical severity in mild and moderate dementia of alzheimer type. *Neuropsychobiology.* 1997;**36**(3):153–158. doi:10.1159/000119375.
33. Fahimi G, *et al.* Index of theta/alpha ratio of the quantitative electroencephalogram in Alzheimer's disease: a case-control study. *Acta Med Iran.* 2017;**55**(8):502–506.
34. Kam K, *et al.* Sleep oscillation-specific associations with Alzheimer's disease CSF biomarkers: Novel roles for sleep spindles and tau. *Mol Neurodegener.* 2019;**14**(1):1–12. doi:10.1186/s13024-019-0309-5.
35. Winer JR, *et al.* Sleep as a potential biomarker of tau and -amyloid burden in the human brain. *J Neurosci.* 2019;**39**(32):6315–6324. doi:10.1523/JNEUROSCI.0503-19.2019.
36. Vazquez J, *et al.* Rapid communication. *Am J Phys Regul Integr Comp Physiol.* 2001;**280**(2):R598–R601. doi:10.1016/S0016-5085(77)80340-5.
37. Mufson EJ, *et al.* Cholinergic system during the progression of Alzheimer's disease: therapeutic implications. *Expert Rev Neurother.* 2008;**8**(11):1703–1718. doi:10.1586/14737175.8.11.1703.
38. Babiloni C, *et al.* Hippocampal volume and cortical sources of EEG alpha rhythms in mild cognitive impairment and Alzheimer disease. *Neuroimage.* 2009;**44**(1):123–135. doi:10.1016/j.neuroimage.2008.08.005.
39. Klimesch W. EEG alpha and theta oscillations reflect cognitive and memory performance: a review and analysis. *Brain Res Rev.* 1999;**29**(2-3):169–195. doi:10.1016/s0165-0173(98)00056-3.
40. Moretti DV, *et al.* Relationship between EEG Alpha3/Alpha2 ratio and the nucleus accumbens in subjects with mild cognitive impairment. *J Neurol Neurophysiol.* 2013;**04**(02):2–7. doi:10.4172/2155-9562.1000149.
41. Moe KE, *et al.* Sleep/wake patterns in Alzheimer's disease: relationships with cognition and function. *J Sleep Res.* 1995;**4**(1):15–20. doi:10.1111/j.1365-2869.1995.tb00145.x.
42. Scally B, *et al.* Resting-state EEG power and connectivity are associated with alpha peak frequency slowing in healthy aging. *Neurobiol Aging.* 2018;**71**:149–155. doi:10.1016/j.neurobiolaging.2018.07.004.
43. Grandy TH, *et al.* Peak individual alpha frequency qualifies as a stable neurophysiological trait marker in healthy younger and older adults. *Psychophysiology.* 2013;**50**(6):570–582. doi:10.1111/psyp.12043.
44. Tanabe S, *et al.* Cohort study of electroencephalography markers of amyloid-Tau-neurodegeneration pathology. *Brain Commun.* 2020;**2**(2):1–10. doi:10.1093/braincomms/fcaa099.
45. Liu S, *et al.* Sleep spindles, K-complexes, limb movements and sleep stage proportions may be biomarkers for amnestic mild cognitive impairment and Alzheimer's disease. *Sleep Breath.* 2020;**24**(2):637–651. doi:10.1007/s11325-019-01970-9.
46. Taillard J, *et al.* Non-REM sleep characteristics predict early cognitive impairment in an aging population. *Front Neurol.* 2019;**10**(March):1–13. doi:10.3389/fneur.2019.00197.
47. Montez T, *et al.* Altered temporal correlations in parietal alpha and prefrontal theta oscillations in early-stage Alzheimer disease. *Proc Natl Acad Sci USA.* 2009;**106**(5):1614–1619. doi:10.1073/pnas.0811699106.
48. Prichep LS, *et al.* Prediction of longitudinal cognitive decline in normal elderly with subjective complaints using electrophysiological imaging. *Neurobiol Aging.* 2006;**27**(3):471–481. doi:10.1016/j.neurobiolaging.2005.07.021.
49. Ktonas PY, *et al.* Potential dementia biomarkers based on the time-varying micro structure of sleep EEG spindles. *Annu Int Conf IEEE Eng Med Biol - Proc.* 2007:2464–2467. doi:10.1109/IEMBS.2007.4352827.
50. Chiang AKI, *et al.* Age trends and sex differences of alpha rhythms including split alpha peaks. *Clin Neurophysiol.* 2011;**122**(8):1505–1517. doi:10.1016/j.clinph.2011.01.040.
51. Carrier J, *et al.* Sleep slow wave changes during the middle years of life. *Eur J Neurosci.* 2011;**33**(4):758–766. doi:10.1111/j.1460-9568.2010.07543.x.
52. Besthorn C, *et al.* Discrimination of Alzheimer's disease and normal aging by EEG data. *Electroencephalogr Clin Neurophysiol.* 1997;**103**(2):241–248. doi:10.1016/s0013-4694(97)96562-7.
53. Neto E, *et al.* EEG spectral features discriminate between Alzheimer's and vascular dementia. *Front Neurol.* 2015;**6**:1–9. doi:10.3389/fneur.2015.00025.
54. Yener GG, *et al.* Quantitative EEG in frontotemporal dementia. *Clin EEG Neurosci.* 1996;**27**(2):61–68. doi:10.1177/155005949602700204.
55. Bonanni L, *et al.* EEG comparisons in early Alzheimer's disease, dementia with Lewy bodies and Parkinson's disease with dementia patients with a 2-year follow-up. *Brain.* 2008;**131**(3):690–705. doi:10.1093/brain/awm322.
56. Briel RCG, *et al.* EEG findings in dementia with Lewy bodies and Alzheimer's disease. *J Neurol Neurosurg Psychiatry.* 1999;**66**(3):401–403. doi:10.1136/jnnp.66.3.401.